Atomic line emission and high-order harmonic generation in argon driven by 4-MHz sub-μJ laser pulses

Alexander Blättermann,[1,2,*] Cheng-Tien Chiang,[2,1] and Wolf Widdra[1,2,†]

[1]*Institute of Physics, Martin-Luther-Universität Halle-Wittenberg, Von-Danckelmann-Platz 3, D-06120, Halle (Saale), Germany*

[2]*Max Planck Institute of Microstructure Physics, Weinberg 2, 06120 Halle, Germany*

(Received 31 October 2013; published 3 April 2014)

We report on the coexistence of atomic line emission (ALE) and high-order harmonic generation (HHG) from argon with experimental conditions bridging the multiphoton and tunnel ionization regimes. Driven by sub-μJ femtosecond laser pulses in tight-focusing geometry, characteristic spectra of ALE from highly excited neutral argon as well as from singly ionized argon are detected in the presence of the harmonics. The results are discussed with respect to the electronic structure of argon and the phase-matching condition of the HHG process.

DOI: 10.1103/PhysRevA.89.043404 PACS number(s): 42.65.Ky, 42.65.Re

I. INTRODUCTION

High-order harmonic generation (HHG) is a process in which strong laser pulses with low photon energy, down to the midinfrared region, are converted into bursts of high-energy radiation ranging from the extreme ultraviolet up to hard x ray [1,2]. The celebrated combination of HHG-based light sources with varieties of spectroscopy and microscopy methods allows ultimate time resolution in experiments and real-time observation of ultrafast electron dynamics in general [3]. In the simplified picture of the HHG process, a strong electric field, more than several V/Å, from a driving laser is required to trigger tunnel ionization [4]. This marks a HHG threshold at incident laser peak intensity around 10^{13} W/cm^2. The demand to build a HHG source of the highest possible repetition rate requires therefore detailed knowledge of the onset of the tunnel ionization regime. It has been reported that the threshold intensity for HHG could be greatly reduced by several orders of magnitude using field enhancement in plasmonic nanostructures [5,6]. However, the first exciting results demonstrated by Kim *et al.* [5] could not be reproduced by other groups and the observed emission of vacuum-ultraviolet light was later identified as atomic line emission (ALE) [7,8].

The ALE is usually dominated by the HHG signals when the process is driven by mJ laser pulses from amplified laser systems at low repetition rate [2]. The recent observation of ALE driven by a weak laser field [7,8] signifies more than a technical issue of discriminating ALE from HHG features when they have comparable intensity. From the fundamental physical point of view, the observation is relevant to the transition region between multiphoton and tunnel ionization regimes where the ac-Stark shift and resonances can take place [9–11]. This transition occurs when the Keldysh parameter γ, the ratio of the time scale for tunnel ionization to the period of the incident laser field [12], is close to unity. In a simplified picture, tunnel ionization needs to compete with the oscillating optical electric field, since at a higher frequency the field switches its direction earlier, before the electron tunnels through the dynamically distorted ionization potential. At high field strength and low frequency, $\gamma < 1$, the tunnel ionization dominates, corresponding to experiments showing dominant HHG spectra. At lower field strength and higher frequency, γ goes beyond unity and multiphoton ionization from weakly perturbed atomic states comes into play, leading to the emission of characteristic ALE spectra.

In this paper, we investigate for $\gamma \approx 1$ the coexistence of ALE and HHG from an argon jet driven by femtosecond laser pulses of 650 nJ at 4 MHz repetition rate. In strong contrast to previous studies [8], which showed only either dominant HHG features driven by mJ pulses at several kHz repetition rate or ALE driven by nJ pulses at MHz, we observe the clear coexistence of ALE and HHG processes under otherwise identical experimental conditions. By comparing the ALE spectra with the electronic structure of argon atoms, we assign the ALE features to emission from highly excited neutral argon atoms and singly charged argon ions. The simultaneous observation of ALE and HHG and the understanding of their relative intensities might be important for the development of low-power, but high repetition rate, HHG sources which operate just above the transition regime for $\gamma \approx 1$. As a tool, the observation of ALE might allow one to locate the crossing condition of the μm gas jet and the μm laser focus when the optimal HHG conditions are not yet met. But more essentially, the clear separation of both effects is necessary to assign the HHG radiation under threshold conditions.

HHG sources with MHz repetition rates are essential for the design of laser-based vacuum-ultraviolet light source in electron-based spectroscopy and microscopy, where repetition rate significantly beyond traditional kHz Ti:sapphire amplifier systems [13,14] is necessary. By far, as an alternative to our approach using a sub-μJ laser oscillator at MHz, HHG experiments at this high repetition rate require either intricate high-power fiber laser systems [15–18] or an additional complex resonant cavity for field enhancement [19–21].

II. EXPERIMENTAL SETUP

In Fig. 1(a), an overview of the setup is shown. To drive HHG, we used the output of a Ti:sapphire oscillator with its cavity extended by a Herriott-type multipass cell [22,23]. The

*Present address: Max Planck Institute for Nuclear Physics, Saupfercheckweg 1, 69117 Heidelberg, Germany; alexander.blaettermann@mpi-hd.mpg.de

†Corresponding author: wolf.widdra@physik.uni-halle.de

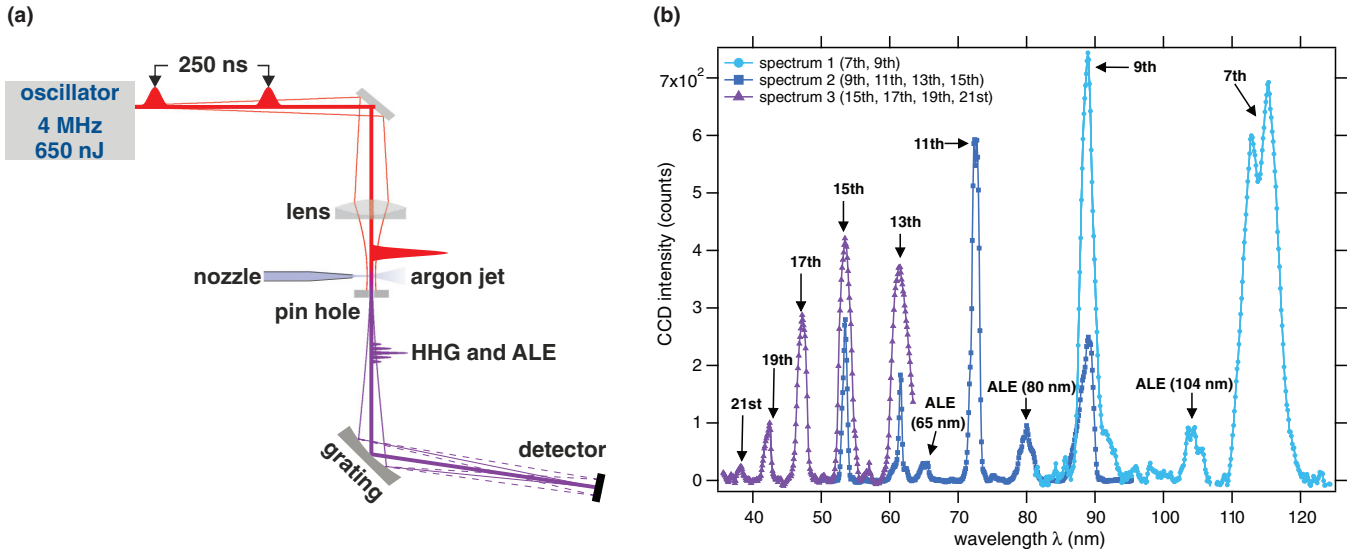

FIG. 1. (Color online) (a) Setup of experiments. (b) Spectra of the generated radiation from argon, measured for 7.5 s for spectra 1 and 2, and 60 s for spectrum 3. The three spectra are measured with different diffraction angles by which the grating is rotated. A smooth background was subtracted from the spectra. The order of the harmonics and the atomic lines (ALE) with their wavelength are indicated.

laser output has a central wavelength around 800 nm, and a pulse energy of 650 nJ with 50 fs pulse duration at 4 MHz repetition rate. An achromatic lens focuses the laser beam into an argon gas jet emerging from a glass capillary with 30 μm orifice and a backing pressure of 3 to 4 bar. The focal length is about 50 mm, which results in a beam-waist diameter of around 5 μm. These focus parameters are in strong contrast to the conventional HHG setups using amplified laser systems with μJ to mJ pulse energy, in which a sufficient intensity can still be provided by a much larger focus size. In our case, the peak intensity at the focus is estimated to be 7×10^{13} W/cm^2. The emitted vacuum-ultraviolet light is diffracted and focused onto an imaging detector by a toroidal grating. Due to the diffraction geometry, the longest wavelength that can be observed is around 120 nm and a wide spectral range can be detected upon rotation of the grating. The diffracted HHG pulses are stretched to a temporal width of 1 to 2 ps according to the line density of the grating and the estimated beam-spot size on the grating. Details of the setup are described elsewhere [24].

III. RESULTS

Figure 1(b) shows spectra of vacuum-ultraviolet light generated from an argon jet with a backing pressure of 4 bar. In the spectra, the harmonics of the driving laser field are indicated by their harmonic order and the additional features are attributed to atomic lines (ALE) of argon. The photon flux is estimated to be 2×10^4 photons/s for the 13th harmonic with an assumed 10% efficiency of the detector. This flux is about 4 orders of magnitude lower than that of a conventional HHG setup driven by amplifier laser systems [14].

By using the cutoff in the HHG spectra as a reference, we can estimate the Keldysh parameter γ in our experiment as the following. The HHG spectra extend up to the 17th harmonic and show a cutoff around the 19th harmonic with a photon energy of 29.5 eV (E_{cutoff}). According to the empirical cutoff law of HHG [25], the ponderomotive energy (U_P) of electrons in the laser field can be estimated by $E_{\text{cutoff}} = I_P + 3.17U_P$. Here, I_P is the ionization potential of the neutral argon atom of 15.8 eV. U_P is estimated to be 4.3 eV and the peak intensity at the laser focus is estimated to be around 7.3×10^{13} W/cm^2. This peak intensity is in reasonable agreement with our estimation by the focus spot size. From these, we estimate the Keldysh parameter $\gamma \approx 1.4$, which is in the transition region between the multiphoton and tunnel ionization regimes.

As a crosscheck for the assignment of ALE and HHG, we used xenon instead of argon as the generation medium, and harmonics up to the 13th order were observed with higher intensity, whereas the ALE features at 65, 80, and 104 nm wavelength were not observed (data not shown). This suggests that the assigned ALE features are related to the characteristic electronic structure of argon atoms and ions.

The detailed spectrally resolved structure of the ALE is shown in Fig. 2. Figures 2(a) and 2(b) display the two-dimensional diffraction pattern and Fig. 2(c) shows the corresponding line profiles. In the presented spectral range, the 9th, 11th, and 13th harmonics dominate, but additional features appear at about 64 and 80 nm, which we resolve with high resolution. In Fig. 2(b), the diffraction pattern of the generated radiation is measured under identical conditions, except for a reduced exposure time as in Fig. 2(a), and the argon gas jet is displaced by about 30 μm away from the lens along the light propagation axis. As clearly shown by the comparison between the line profiles in Fig. 2(c), the intensity of the 11th harmonic was about tripled from Figs. 2(a) to 2(b), whereas the ALE features completely vanish. This observation shows directly the very different generation conditions for ALE and HHG.

IV. DISCUSSION

In general, the identification of specific ALE transitions simultaneously in HHG experiments is not straightforward

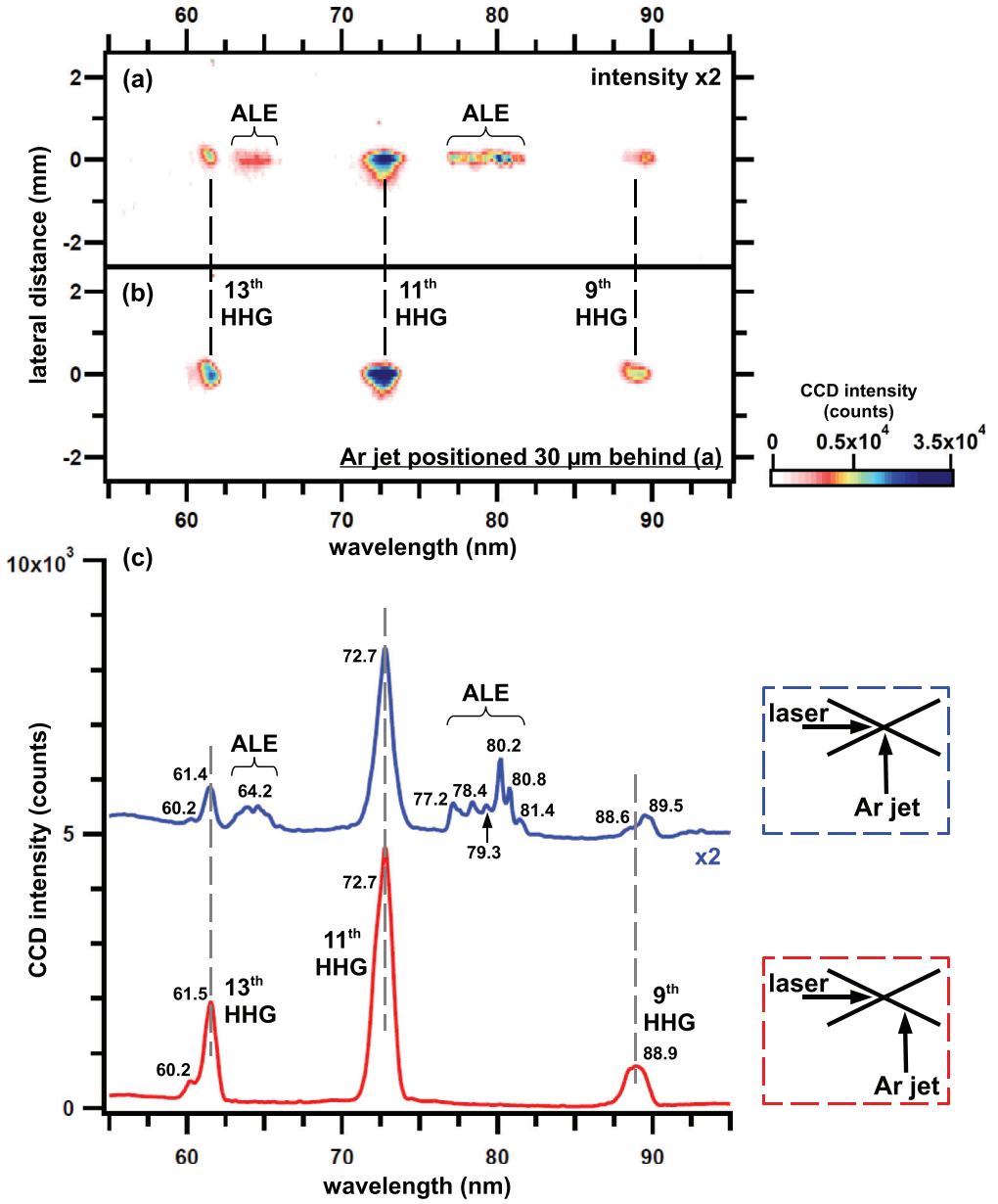

FIG. 2. (Color online) (a),(b) The diffraction patterns of generated vacuum-ultraviolet radiation for two different argon jet positions. In (a), the argon jet is positioned 30 μm closer toward the incident laser beam than in (b). (c) The averaged line profiles from (a), blue curve, and (b), red curve. A constant background in the line profile is subtracted. For clarity, the blue curve is vertically shifted. The exposure time for image (a) and (b) is 22 and 11 s, respectively, and a factor 2 should be taken into account when comparing their absolute intensity.

because of the abundance of possible transitions [7] as well as laser-intensity-dependent Stark shifts of the characteristic atomic lines [9–11]. Moreover, the HHG spectra can depend on the generation geometry and the driving laser-pulse energy. It has been shown that different electron trajectories can lead to splittings of the odd harmonic spectral features; however, at sub-μJ pulse energies in tight-focusing geometry, significant splittings are absent according to the detailed study by Heyl *et al*. [26]. For comparison with the experimental spectra, we show in Fig. 3 the atomic transitions of neutral argon reported in the literature summarized by the Grotrian diagram [27–30]. Here the excited atomic levels of neutral argon are indicated with their energies relative to the ground-state $[\mathrm{Ne}]3s^2 3p^6$ electronic configuration. Selected optical transitions from these excited states to the ground state are sketched and labeled with the emitted wavelength (λ).

Comparing the observed vacuum-ultraviolet spectra in Fig. 1(b) with the energy diagram in Fig. 3(a), we can assign the ALE features near 80 and 104 nm to atomic transitions in neutral argon atoms. The ALE feature near 104 nm agrees well with the transitions from the excited states $[\mathrm{Ne}]3s^2 3p^5 4s^1$ at about 12 eV ($\lambda = 104.8, 106.7$ nm) to the ground state. These transitions were also observed in Ref. [8] when argon is driven by mJ laser pulses at 1 kHz. Furthermore, the feature near 80 nm with fine-scale spectra features revealed in Fig. 2(c) can be related to transitions from highly excited states near the ionization threshold (I_P), i.e., $[\mathrm{Ne}]3s^2 3p^5 ns^1$ with $n \geqslant 6$ and $[\mathrm{Ne}]3s^2 3p^5 nd^1$ with $n \geqslant 4$, to the ground state.

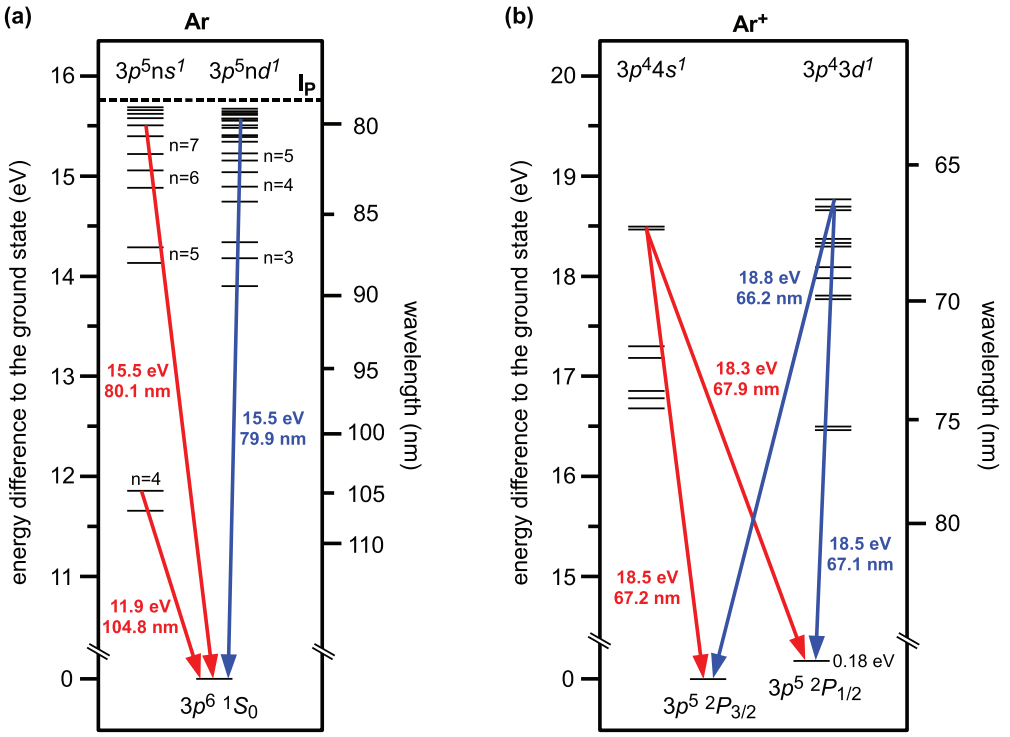

FIG. 3. (Color online) The relevant Grotrian diagrams of (a) a neutral argon atom [27–29] and (b) a singly ionized argon ion [28,30] for the observed atomic emission lines. Excited states are shown with the energy (left axis) and emitted wavelength (right axis) in an optical transition to the ground states. Examples for dipole allowed transitions are indicated by the arrows labeled with the wavelength of emitted radiation. In (a), the ionization energy (I_P) for a singly charged ion is marked by the dashed line.

A closer look at the fine-scale spectra feature near 80 nm in Fig. 2(c) reveals its extension down to 77.2 nm. This value is smaller than the corresponding value of the ionization potential (I_P) of 78.8 nm. Since all the $[Ne]3s^23p^5ns^1$ and $[Ne]3s^23p^5nd^1$ bound states must be located below I_P in the argon atom in a field-free environment, we tentatively attribute this deviation to the dynamic Stark effect due to the strong driving laser field. In analogy, comparing the weak ALE feature near 65 nm in Fig. 2(c) with Fig. 3(b), we could assign this feature to transitions of singly charged argon ions from the energetically higher states $[Ne]3s^23p^44s^1$ or $[Ne]3s^23p^43d^1$ to the $[Ne]3s^23p^5$ ground state with wavelength in the range of 66 to 70 nm. According to the experiments of Ackermann *et al.*, the Stark shift depends linearly on the laser intensity with a slope of about 5 meV per 10^{12} W/cm^2 for the $[Ne]3s^23p^54s^1$ to $[Ne]3s^23p^6$ transition driven by a laser at around 500 nm [11]. In our case, this would result in a shift of about 350 meV, which is in good agreement with the experimentally obtained values of the transitions near 104 nm shifted by about 2 nm. In highly excited states, electrons are even more affected by the driving laser field and the energy shift may be even comparable to the ponderomotive energy (U_P) [31].

In our experiments, we could not precisely quantify the magnitude of the Stark shift due to a possible experimental error in the relative wavelength determination of the ALE features. Due to the different directional characteristics of HHG and ALE, a small deviation could result from the different illumination of the diffraction grating. The harmonics will follow the fundamental driving laser beam, whereas the ALE is isotropic. From the observed ALE feature at 104 nm in Fig. 1(b) and the expected transition from $[Ne]3s^23p^54s^1$ at 104.8 nm and 106.7 nm, we can estimate an upper limit of the error of around 2 nm. This size of error can occur when there is a misalignment of around 0.1 mm near the optical axis between the driving laser and the optical components.

After identifying the specific ALE features, we now discuss their dependence on the argon jet position with respect to the laser focus. The atomic transitions are incoherent single-atom processes and the phase difference between emitters does not play any role in ALE. Therefore, it is expected that ALE is most efficient where the excitation is strongest, namely, when the argon jet is placed directly in the laser focus. This simple consideration neglects the dynamic Stark effect, which can shift atomic levels into multiphoton resonance with the incident laser [11]. In contrast, HHG is based on the laser-induced atomic nonlinear polarization and the coherent superposition of the emitted waves from single atoms in the generation medium, i.e., the argon gas jet. As a result of the phase mismatch due to focusing, optical dispersion in the gas, and intrinsic atomic polarization phase shift, the optimized gas jet position is located slightly behind the laser focus [32,33]. In our experiments with sub-μJ pulse energy and tight-focusing geometry, the compensation of the Gouy phase of the focused laser beam by the neutral gas optical dispersion plays an important role [13,14]. As an estimation, the optimal condition for HHG is calculated by numerical simulation of the propagation of the laser-induced polarization and the electric field using the paraxial Helmholtz equation and Green's function method. We estimate an optimum position for the 11th harmonic at about 36 μm behind the laser focus.

According to this value, together with the observed 30 μm shift between the argon jet position for experiments shown in Figs. 2(a) and 2(b), we confirm that the optimum gas jet position for ALE is at the laser focus, as schematically shown in the inset beside Fig. 2(c). This is also consistent with our observation that there exists only one position for maximal ALE intensity when scanning the gas jet position along the laser propagation direction.

V. SUMMARY

To summarize, we observe the coexistence of characteristic atomic line emission (ALE) and high-order harmonic generation (HHG) from argon excited by tightly focused sub-μJ laser pulses at 4 MHz repetition rate. By this, we provide a detailed study of HHG in a rare gas jet at the transition from multiphoton to tunnel ionization regimes ($\gamma \approx 1$). The identified ALE features are assigned to transitions in neutral argon atoms from the optically excited $3p^5 4s$ state and higher excited states near the ionization threshold to the $3p^6$ ground state. In addition, there are weak ALE features attributed to transitions in singly charged argon ions from the excited $3p^4 4s^1$ or $3p^4 3d^1$ states to the $3p^5$ ground state. The simultaneously observed HHG spectra extend up to the 21st order with a photon energy of about 32 eV. Due to the phase-matching condition involved in HHG, the relative weighting of harmonics and atomic lines can be controlled by the gas jet positioning with respect to the incident laser focus. We demonstrate a straightforward way to identify and control the contributions of ALE relative to HHG by positioning the gas media relative to the laser focus, which could be important for the design of HHG experiments where the contribution of ALE should be minimized [5–8].

ACKNOWLEDGMENTS

Technical support from R. Kulla, M. Kiel, and M. Schröder, as well as support and fruitful discussion with F. O. Schumann and J. Kirschner, are gratefully acknowledged.

[1] A. McPherson, G. Gibson, H. Jara, U. Johann, T. S. Luk, I. A. McIntyre, K. Boyer, and C. K. Rhodes, J. Opt. Soc. Am. B **4**, 595 (1987).
[2] X. F. Li, A. L'Huillier, M. Ferray, L. A. Lompré, and G. Mainfray, Phys. Rev. A **39**, 5751 (1989).
[3] F. Krausz and M. Ivanov, Rev. Mod. Phys. **81**, 163 (2009).
[4] P. B. Corkum, Phys. Rev. Lett. **71**, 1994 (1993).
[5] S. Kim, J. Jin, Y.-J. Kim, I.-Y. Park, Y. Kim, and S.-W. Kim, Nature (London) **453**, 757 (2008).
[6] I.-Y. Park, S. Kim, J. Choi, D.-H. Lee, Y.-J. Kim, M. F. Kling, M. I. Stockman, and S.-W. Kim, Nat. Photon. **5**, 677 (2011).
[7] M. Sivis, M. Duwe, B. Abel, and C. Ropers, Nature (London) **485**, E1 (2012).
[8] M. Sivis, M. Duwe, B. Abel, and C. Ropers, Nat. Phys. **9**, 304 (2013).
[9] E. Mevel, P. Breger, R. Trainham, G. Petite, P. Agostini, A. Migus, J.-P. Chambaret, and A. Antonetti, Phys. Rev. Lett. **70**, 406 (1993).
[10] R. M. Potvliege and S. Vučić, Phys. Rev. A **74**, 023412 (2006).
[11] P. Ackermann, H. Münch, and T. Halfmann, Opt. Express **20**, 13824 (2012).
[12] L. V. Keldysh, Zh. Eksp. Teor. Fiz. **47**, 1945 (1965) [JETP **20**, 1307 (1965)].
[13] F. Lindner, W. Stremme, M. G. Schätzel, F. Grasbon, G. G. Paulus, H. Walther, R. Hartmann, and L. Strüder, Phys. Rev. A **68**, 013814 (2003).
[14] C. M. Heyl, J. Güdde, A. L'Huillier, and U. Höfer, J. Phys. B **45**, 074020 (2012).
[15] F. J. Furch, S. Birkner, F. Kelkensberg, A. Giree, A. Anderson, C. P. Schulz, and M. J. J. Vrakking, Opt. Express **21**, 22671 (2013).
[16] A. Thai, M. Hemmer, P. K. Bates, O. Chalus, and J. Biegert, Opt. Lett. **36**, 3918 (2011).
[17] J. Boullet, Y. Zaouter, J. Limpert, S. Petit, Y. Mairesse, B. Fabre, J. Higuet, E. Mével, E. Constant, and E. Cormier, Opt. Lett. **34**, 1489 (2009).
[18] A. Vernaleken, J. Weitenberg, T. Sartorius, P. Russbueldt, W. Schneider, S. L. Stebbings, M. F. Kling, P. Hommelhoff, H.-D. Hoffmann, R. Poprawe, F. Krausz, T. W. Hänsch, and T. Udem, Opt. Lett. **36**, 3428 (2011).
[19] E. Seres, J. Seres, and C. Spielmann, Opt. Express **20**, 6185 (2012).
[20] A. Cingöz, D. C. Yost, T. K. Allison, A. Ruehl, M. E. Fermann, I. Hartl, and J. Ye, Nature (London) **482**, 68 (2012).
[21] I. Pupeza, S. H. amd T. Eidam, H. Carstens, D. E. aned J. Weitenberg, P. Rußbüldt, J. Rauschenberger, J. Limpert, T. Udem, A. Tünnermann, T. W. Hänsche, A. Apolonski, F. Krausz, and E. Fill, Nat. Photon. **7**, 608 (2013).
[22] Femtosource scientific XL 650, Femtolasers Produktions GmbH, Vienna, Austria (2011).
[23] D. Herriott and H. J. Schulte, Appl. Opt. **4**, 883 (1965).
[24] C.-T. Chiang, A. Blättermann, M. Huth, J. Kirschner, and W. Widdra, Appl. Phys. Lett. **101**, 071116 (2012).
[25] A. L'Huillier, M. Lewenstein, P. Salières, P. Balcou, M. Y. Ivanov, J. Larsson, and C. G. Wahlström, Phys. Rev. A **48**, R3433 (1993).
[26] C. M. Heyl, J. Güdde, U. Höfer, and A. L'Huillier, Phys. Rev. Lett. **107**, 033903 (2011).
[27] H. Beutler, Z. Phys. **93**, 177 (1935).
[28] J. E. Sansonetti and W. C. Martin, J. Phys. Chem. Ref. Data **34**, 1559 (2005).
[29] L. Minnhagen, J. Opt. Soc. Am. **63**, 1185 (1973).
[30] L. Minnhagen, J. Opt. Soc. Am. **61**, 1257 (1971).
[31] A. L'Huillier, L. A. Lompré, D. Normand, X. Tang, and P. Lambropoulos, J. Opt. Soc. Am. B **6**, 1790 (1989).
[32] C. Winterfeldt, C. Spielmann, and G. Gerber, Rev. Mod. Phys. **80**, 117 (2008).
[33] P. Balcou and A. L'Huillier, Phys. Rev. A **47**, 1447 (1993).